Structure and Ionic Conductivity of Ga and Nb Dual Doped $Li_7La_3Zr_2O_{12}$ Synthesized by Sol-Gel Method

Jun LI [1] *, Fuzhong WANG [2], Leichao MENG [2], Tao GAO [1], Bo LIANG [1], Hang ZHANG [1], Meili CUI [1], Xinxin LU [1], Ying CAO [1], Jiyong CHEN [1]

[1] *School of Aviation and Transportation, Jiangsu College of Engineering and Technology, Nantong 226007, China*
[2] *School of Physics and Electronic Information Engineering, Qinghai Minzu University, Xining 810007, China*

More and more attention has been focused on $Li_7La_3Zr_2O_{12}$ (LLZO) because of its high ionic conductivity and excellent chemical stability. It is of great significance to find suitable dopants for locking cubic LLZO and improving the conductivity of Li^+ ions. The uniform nano powder can be obtained by the sol gel synthetic method, which is conducive to maintaining high sintering activity. In this work, Ga and Nb dual doped LLZO solid electrolyte powders were synthesized via sol gel method, and Ga and Nb dual doped LLZO solid electrolyte ceramic were obtained via the traditional solid state sintering method. The phase and microstructure of Ga and Nb co-doped LLZO solid electrolyte were analyzed by combining X-ray diffraction with a scanning electron microscope. The impedance of Ga and Nb dual doped LLZO ($Li_{6.8-3x}Ga_xLa_3Zr_{1.8}Nb_{0.2}O_{12}$ ($0 \leq x \leq 0.3$)) solid electrolyte was measured by the electrochemical workstation, and then the conductivity was calculated. The results show that when the doping amount of Ga is $x = 0.2$, it is a pure cubic LLZO structure with the highest conductivity value of 3.7×10^{-4} S cm^{-1} (tested at room temperature) due to the sample has a high relative density and reaches the optimal Li^+ vacancy concentration.

Keywords: solid state electrolyte, dual doped, conductivity, sol gel.

1. INTRODUCTION

Scientific attention has been focused on lithium ion batteries (LIBs) owing to the supremely outstanding advantages, for example, high energy density, high working voltage, good cycle performance, light weight, no pollution, no memory effect, and small self-discharge [1 – 3]. Nowadays, LIBs, as the main energy storage and power supply equipment, have developed rapidly and brought many conveniences to human society [4, 5]. At present, LIBs for commercial use liquid electrolytes usually, which exist safety problems such as leakage, flammability and explosion. In addition, the current energy density of LIBs is still unable to meet the needs of long-distance travel. Solid state batteries are considered to solve the problems of safety and energy density [6 – 8]. As the core component of a solid lithium battery, the properties of solid electrolyte is directly related to the performance of the whole battery.

Solid electrolytes consist of two different types. One is a polymer electrolyte and another is an inorganic electrolyte [9 – 14]. Compared with polymer solid electrolyte, inorganic electrolyte can maintain chemical stability in a wider voltage window and operating temperature range. The battery based on inorganic solid electrolyte has higher safety characteristics and gradually attracted more attention. Among many inorganic solid electrolytes, $Li_7La_3Zr_2O_{12}$ (LLZO) with garnet structure has attracted more and more scientific attention because of the high conductivity, excellent thermal performance, and excellent chemical and electrochemical stability [15, 16].

Two different phases: tetragonal and cubic is existed in LLZO. The conductivity of cubic LLZO is several hundred times larger than that of tetragonal LLZO. The cubic phase can be obtained by partial high-valent substitution. Sharifi et al. synthesized $Li_{7-3x}Al_xLa_3Zr_2O_{12}$ garnet by replacing Li^+ with Al^{3+}, and the electrolyte shows a cubic phase with higher ionic conductivity [17]. Birkner et al. studied the relationship between thermodynamic stability and conductivity of $Li_{7-3x}Ga_xLa_3Zr_2O_{12}$. The undoped $Li_{7-3x}Ga_xLa_3Zr_2O_{12}$ was assignable to the tetragonal phase, while Ga-doped LLZO electrolyte samples were crystallized in the cubic phase and a maximum conductivity was obtained at $x = 0.529$ [18]. Gao designed a Ti-doped LLZO combining electronic conducting and ionic conducting, and the electrolyte shows high ionic conductivity of the cubic phase [19]. In addition, Ta^{5+} can replace Zr^{4+} to lock the cubic phase for obtaining an electrolyte with high ionic conductivity [20].

It is an important research direction for finding suitable doping to get cubic LLZO and improve the conductivity of Li^+ ions. In this direction, LLZO with high ionic conductivity was obtained by partially replacing Zr^{4+} with Nb^{5+}. Ohta synthesized $Li_{7-x}La_3(Zr_{2-x}, Nb_x)O_{12}$ by solid state reaction, and the conductivity was measured. The conductivity increased with the content of Nb, and reached a maximum value (8×10^{-4} S cm^{-1}) [21]. In addition, double doping can further adjust the structure and improve ionic conductivity. Buannic et al. designed an innovative dual substitution to increase the mobility of Li^+ in garnet-type LLZO solid electrolytes. Ga^{3+} as the first dopant cation is used to replace Li^+ to stabilize the high conductivity cubic phase. At the same time, Sc^{3+} as the second cation is populated on the Zr sites, to further fine-

---

* Corresponding author. Tel.: +86-17826152287; fax: +86-0513-81050109. E-mail: *lijun7239@nuaa.edu.cn* (J. Li)

tune the structure to get a higher conductivity. The $Li_{7-3x+y}Ga_xLa_3Zr_{2-y}Sc_yO_{12}$ shows the maximum values of 1.8×10^{-3} S cm^{-1} at 300 K, which is the largest value so far [22].

In addition to the doping, the microstructure of ceramics is also the key factor affecting the properties of LLZO. LLZO powder commonly used for sintering ceramics is synthesized by solid state reaction [23]. The grain size synthesized is relatively large by this method, which is unfavourable to obtain a good sintering activity. Sintering of electrolyte ceramics from LLZO powder by solid state reaction needs to take a long sintering time at high temperature and it is easy to produce an impure phase. In contrast, sol gel method can provide molecular level mixing and produce nano powder, which is conducive to prepare ceramics with higher purity at not only low sintering temperature but also short sintering time [24, 25].

In this paper, a new doped LLZO was synthesized by sol gel method, in which Ga^{3+} and Nb^{5+} were used to partially replace Li^+ and Zr^{4+} in $Li_7La_3Zr_2O_{12}$. The new doping method is used for increasing the conductivity, and the doped LLZO with a smaller particle size is obtained from the sol gel method, which is conducive to maintaining high sintering activity. The preparation of Ga^{3+} and Nb^{5+} co-doped $Li_7La_3Zr_2O_{12}$ and the addition of Ga on the morphology and ionic conductivity of $Li_{6.8}La_3Zr_{1.8}Nb_{0.2}O_{12}$ were systematically studied.

2. EXPERIMENT

2.1. Preparation of powders and ceramics of $Li_{6.8-3x}Ga_xLa_3Zr_{1.8}Nb_{0.2}O_{12}$ ($0 \leq x \leq 0.3$)

CH_3COOLi, $C_6H_9O_6La \cdot xH_2O$, $C_5H_8N_2O_{15}Zr_2$, $Ga(NO_3)_3 \cdot xH_2O$, $C_{10}H_5NbO_2$, $C_6H_8O_7 \cdot H_2O$, $C_2H_6O_2$, were purchased from Macklin Chemical Co. All purchased materials are analytical grade, which can be directly used without any purification.

Ga and Nb Co-doped LLZO powders were synthesized via the sol gel method, and the ceramics of which were prepared by conventional sintering method under normal pressure. CH_3COOLi, $Ga(NO_3)_3 \cdot xH_2O$, $C_6H_9O_6La \cdot xH_2O$, $C_5H_8N_2O_{15}Zr_2$, $C_{10}H_5NbO_2$ were prepared according to the molar ratio of $(6.8-3x):x:3:0.9:0.2$. Another 10 % excess CH_3COOLi was supplied for compensating loss of lithium in the process of sintering.

Two different solutions are needed for synthesizing $Li_{6.8-3x}Ga_xLa_3Zr_{1.8}Nb_{0.2}O_{12}$ ($0 \leq x \leq 0.3$) powder. CH_3COOLi, $Ga(NO_3)_3 \cdot xH_2O$, $C_6H_9O_6La \cdot xH_2O$, $C_5H_8N_2O_{15}Zr_2$ were added into the $C_6H_8O_7 \cdot H_2O$ solution in turn according to the molar ratio, and the content of $C_6H_8O_7 \cdot H_2O$ was twice the total molar amount of cations in the $Li_{6.8-3x}Ga_xLa_3Zr_{1.8}Nb_{0.2}O_{12}$ ($0 \leq x \leq 0.3$). Then $NH_3 \cdot H_2O$ was added into the above solution until pH $\approx$ 7 for obtaining the first solution. $C_{10}H_5NbO_2$ was dissolved in $C_2H_6O_2$ for obtaining a second solution, and the amount of $C_2H_6O_2$ was the same molar amount of $C_6H_8O_7 \cdot H_2O$. First of all, the two above solutions were mixed and stirred to prepare a transparent uniform solution at room temperature for 24 hours. Secondly, the being uniform solution was evaporated at 100 °C for 3 h before dried for forming yellow gels at 250 °C for 3 h. Finally, the gels were ground

and then calcined in an air atmosphere at 800 °C for 8 h to obtain $Li_{6.8-3x}Ga_xLa_3Zr_{1.8}Nb_{0.2}O_{12}$ ($0 \leq x \leq 0.3$) powders. The powders were pressed into pellets with a diameter of 10mm, and then the pellets were sintered for synthesizing ceramics by cover in master powders at 1100 °C for 8 h.

2.2. Characterization

X-ray diffraction (XRD) was supplied for determining the phase of the prepared samples, the model of which was D8 Advance purchased from Germany. The radiation source tested is Cu Kα in the scanning range of 2θ from 10° to 70°. The morphologies of electrolyte samples were analyzed by scanning electron microscope (SEM), the model of which is HITACHIS-4800 purchased from Japan.

The impedance of samples was measured by electrochemical impedance (EIS), and the ionic conductivity was calculated. The equipment used for the EIS test was CHI660E (Shanghai Chenhua) electrochemical workstation. The sample was polished and coated with silver (as a blocking electrode) to be tested, the test frequency range was $0.01 \sim 10^6$ Hz, and the AC signal voltage amplitude was 10 mV. The ionic conductivity σ can be calculated by substituting the impedance value R obtained from the EIS test into Eq. 1:

$$\sigma = L/(R \times S), \tag{1}$$

where L represented the thickness of the electrolyte sample and S represented the area of the blocking electrode.

3. RESULTS AND DISCUSSION

Fig. 1 is the X-ray diffraction diagram of $Li_{6.8-3x}Ga_xLa_3Zr_{1.8}Nb_{0.2}O_{12}$ ($x = 0.3$) powder prepared by calcination at 800 °C for 8 hours. The synthesized product is a cubic structure with high ionic conductivity according to the PDF card (No.45-0109). In addition, the diffraction peak of 28.6° appears, which is an index to impurity phase pyrochlore structure $La_2Zr_2O_7$ according to the PDF card (No.71-2363). The impurity product is the intermediate in the processing of synthesizing cubic LLZO, which can be removed by heating at a temperature above 700 °C for a long time [26].
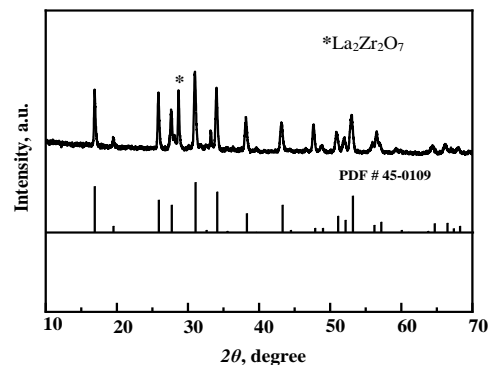
Fig. 1. XRD spectra of $Li_{5.9}Ga_{0.3}La_3Zr_{1.8}Nb_{0.2}O_{12}$ powder prepared at 800 °C for 8 h

Fig. 2 shows the SEM of $Li_{6.8-3x}Ga_xLa_3Zr_{1.8}Nb_{0.2}O_{12}$ ($x = 0.3$) powder prepared at 800 °C for 8 h. It can be seen from Fig. 2 b that the size of the single crystal of the prepared solid electrolyte LLZO material is about 100 nm,

which is related to the preparation process. The small particles not only help to improve the sintering activity, but also can reduce the temperature and holding time during the sintering process. The pellet samples in this work can be sintered at 1100 °C for 8 h.
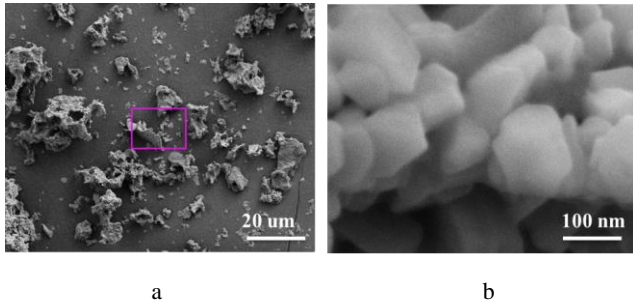
Fig. 2. SEM images of $Li_{5.9}$ $Ga_{0.3}La_3Zr_{1.8}Nb_{0.2}O_{12}$ powder prepared at 800 °C for 8 h: a – overall diagram; b – partial enlarged diagram

The above sintering temperature (1100 °C) is significantly lower than that of the powder synthesized via the traditional solid state reaction method (about 1200 °C). In addition, compared with the long sintering time (about 36 hours) of the powder synthesized via the traditional solid state reaction method [27], and the sintering time of the synthesized powder is shorter (only 8 hours) in this work, indicating the high sintering activity of powders, which is benefits from the nanometer size of the powder prepared via the sol gel method. In addition, Fig. 2 a shows that the particle size of the powder is mostly $1-5$ µm, indicating that there are many particles agglomerations due to the large surface energy of nanometer powder resulting in the phenomenon.

Fig. 3 shows the XRD diagrams of ceramics of $Li_{6.8-3x}Ga_xLa_3Zr_{1.8}Nb_{0.2}O_{12}$ $(0 \leq x \leq 0.3)$ electrolyte at sintering conditions of combining 1100 °C with 8h. In the case of $x = 0$, any diffraction peak of the sample corresponds to cubic phase LLZO (No.45-0109 of PDF card).
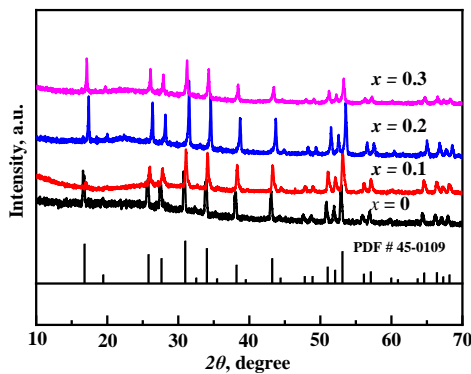
Fig. 3. XRD patterns of ceramics of $Li_{6.8-3x}$ $Ga_xLa_3Zr_{1.8}Nb_{0.2}O_{12}$ $(0 \leq x \leq 0.3)$ electrolytes sintered at 1100 °C for 8 h

The above result shows that the cubic structure of LLZO can be stabilized at room temperature by single-doped Nb element occupying the Zr site, which is consistent with others [28]. Previous studies showed that no any element doping will only get tetragonal phase LLZO at room temperature [29]. The conductivity of cubic phase LLZO exhibits higher conductivity compared to

tetragonal phase LLZO, which is a hundred times higher. In summary, the sample has higher ionic conductivity through Nb element occupying the Zr site synthesized in this work. Ga as a second cation is used to occupy the Li sites to further fine-tune the structure to get a higher conductivity. Proper Ga doping can motivate more lithium ions to take part in conduction and get the larger size of the migration pathway which benefits increasing mobility. Furthermore, a higher Coulombic repulsion can be achieved between Ga^{3+} and Li^+ benefiting from activating more lithium ions than that between lithium ions. All samples with added Ga ($Li_{6.8-3x}Ga_xLa_3Zr_{1.8}Nb_{0.2}O_{12}$ $(0.1 \leq x \leq 0.3)$) are still cubic phase LLZO structure, and there is no impurity phase. It's worth noting that the peak intensities of the XRD pattern for x=0.1 compound at about 17 degrees are different from others, which may be due to a loss of lithium content [30]. Fig.4 shows the fitting profile of the XRD result of $Li_{6.2}Ga_{0.2}La_3Zr_{1.8}Nb_{0.2}O_{12}$. All diffraction peaks can be indexed with the cubic phase LLZO, and Ga occupies Li sites [31].
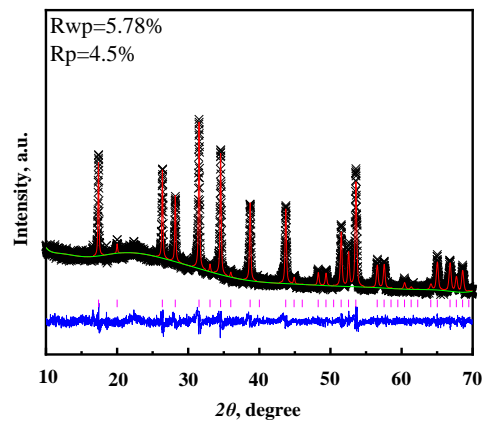
**Fig. 4.** Fitting profile of XRD result of $Li_{6.2}Ga_{0.2}La_3Zr_{1.8}Nb_{0.2}O_{12}$

The diffraction peaks of samples ($Li_{6.8-3x}Ga_xLa_3Zr_{1.8}Nb_{0.2}O_{12}$ $(0.1 \leq x \leq 0.3)$) slightly shift to the right, because the smaller Ga^{3+} ($r = 0.62$ Å) replaces the larger Li^+ (r = 0.76 Å), resulting in the decrease of lattice constant and the shift of peak position to the right. The above results show that the samples not only keep the cubic phase with high ionic conductivity, but also obtain minor structural changes after adding the Ga element, which is benefitial for further enhancing the ionic conductivity (this result is confirmed in the following text).

Fig. 5 is the SEM diagrams of the fracture surface of $Li_{6.8-3x}Ga_xLa_3Zr_{1.8}Nb_{0.2}O_{12}$ $(0 \leq x \leq 0.3)$ ceramic solid electrolyte samples. The particle size of the $x = 0$ electrolyte sample is distributed from 2 to 22 µm, and the average size is 11 µm. In addition, there are a lot of holes between grains. When the doping amount of Ga reaches $x = 0.1$ ($Li_{6.5}Ga_{0.1}La_3Zr_{1.8}Nb_{0.2}O_{12}$), the grain size of the sample begins to decrease, which is distributed between $1-10$ µm, and the average grain size is 6 µm. In addition, the holes between grains gradually decrease and become smaller. When the doping amount of Ga further increases ($x = 0.2$, $x = 0.3$), a large number of grains larger than 20 µm appear in the sample. The holes on the samples have basically disappeared. In addition, a cross-section of the sample presents a transgranular structure, which also

confirms the enhanced contact between grains. These results show that an appropriate amount of Ga-Nb co-doping can effectively improve the relative density of prepared ceramics. The increasing relative density is beneficial to improving ionic conductivity.
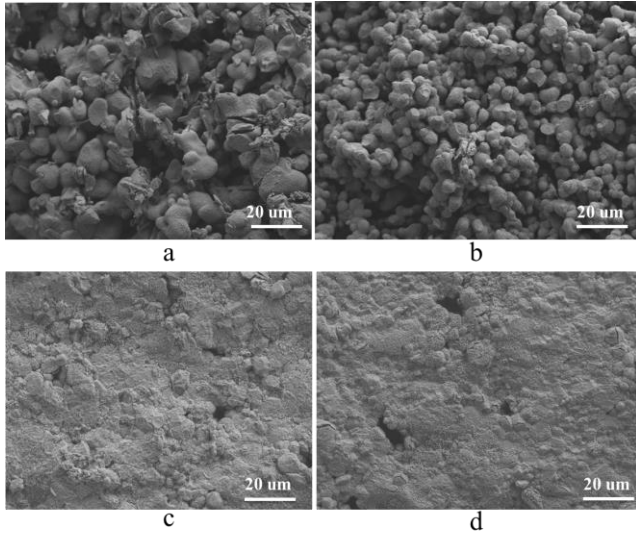
Fig. 5. SEM of ceramics section of $Li_{6.8-3x}Ga_xLa_3Zr_{1.8}Nb_{0.2}O_{12}$ ($0 \leq x \leq 0.3$) electrolytes sintered at 1100 °C for 8 h: $a-x = 0$; $b-x = 0.1$; $c-x = 0.2$; $d-x = 0.3$

Generally speaking, high ionic conductivity is the key to ensure that the electrolyte can be used in lithium batteries. The AC impedance spectrum of $Li_{6.8-3x}Ga_xLa_3Zr_{1.8}Nb_{0.2}O_{12}$ ($0 \leq x \leq 0.3$) solid electrolyte sample is shown in Fig. 6. As can be seen from Fig. 6, when the content of Ga is $x = 0$, the ceramic electrolyte shows a typical impedance spectrum.

There are two semicircles in the middle and high frequency, representing the grain impedance and grain boundary impedance respectively. Furthermore, there is a long linear segment related to the blocking electrode in the low frequency. The total resistance value is the sum of grain impedance and grain boundary impedance. As shown in Fig. 6, with the increase of Ga, the two semicircles (Fig. 6 a and b) in the middle and high frequency gradually combined into a semicircle (Fig. 6 c and d), which indicates the increasing of Ga content reducing the grain interface resistance value. From the SEM results (Fig. 5), the result indicates that the addition of Ga is conducive to the increase of sample density, thus reducing the grain boundary resistance value. Notably, the rapid resistance value decreased by more than an order of magnitude from $x = 0.1$ to $x = 0.2$ due to the significant improvement of relative density (from Fig. 5.) and the changed structure. Fig. 7 is the total ionic conductivity and impedance of $Li_{6.8-3x}Ga_xLa_3Zr_{1.8}Nb_{0.2}O_{12}$ ($0 \leq x \leq 0.3$). The ionic conductivity values of all samples synthesized in this work are much higher than those of samples without any element doping [32]. The total resistance value first decreases and then increases with the increase of Ga, and reaches the minimum value at $x = 0.2$, which is shown in Fig. 7. In other words, the sample with $x = 0.2$ has the maximum ionic conductivity value. The above results indicate that Ga and Nb dual doping method is beneficial for increasing the conductivity.
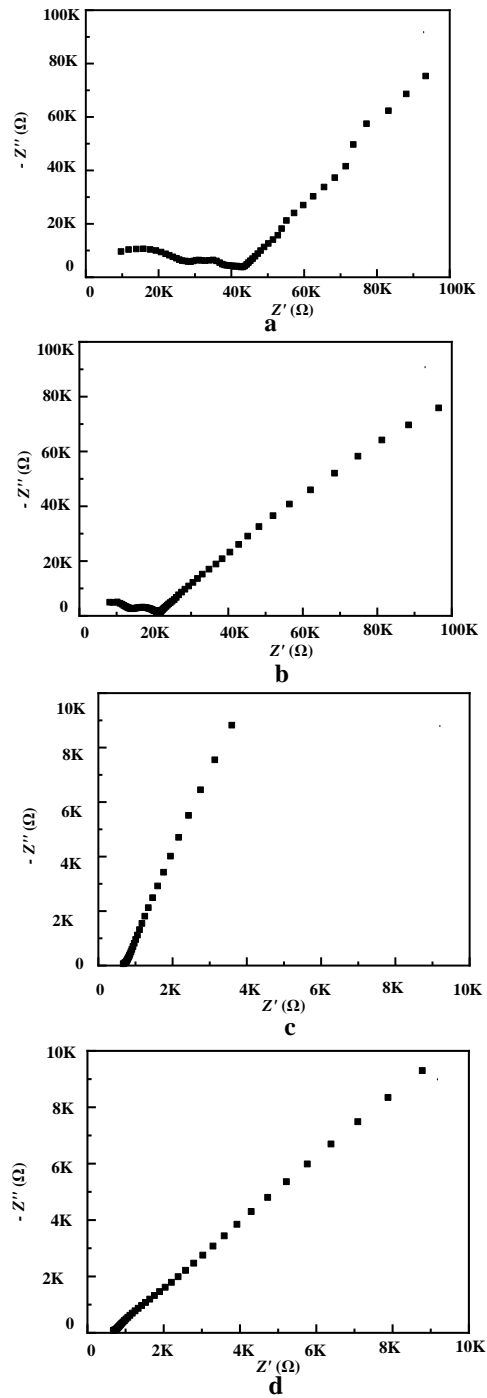
Fig. 6. AC impedance spectrum of $Li_{6.8-3x}Ga_xLa_3Zr_{1.8}Nb_{0.2}O_{12}$ ($0 \leq x \leq 0.3$): $a-x = 0$; $b-x = 0.1$; $c-x = 0.2$; $d-x = 0.3$

The increase of conductivity is due to Ga-Nb double doped samples obtained cubic phase LLZO (from the Fig. 3). In addition, Ga brings not only the change of density, but also the change of Li structure (from the Fig. 3) including vacancies. Although the Li vacancy is beneficial to improve ionic conductivity, there is an optimum value for the Li vacancy. At the optimum value, the sample will have the minimum grain resistance, indicating that the best grain conductivity because the resistance is inversely related to conductivity according to Eq. 1 [33]. A small amount of Ga3+ is introduced in Li6.8La3Zr1.8Nb0.2O12, which leads to an appropriate amount of Li vacancy, thus promoting the movement of Li+.

11
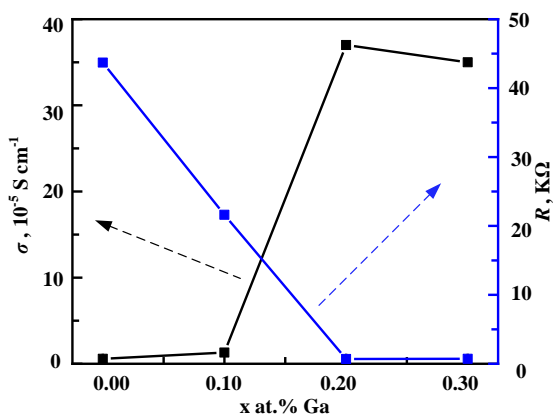
Fig. 7. Total ionic conductivity, impedance of $Li_{6.8-3x}Ga_xLa_3Zr_{1.8}Nb_{0.2}O_{12}(0 \leq x \leq 0.3)$ solid electrolytes

However, the further increase of Li vacancy reduces the content of mobile Li^+, resulting in the decrease of grain conductivity. Therefore, the total resistance value of the sample with $x = 0.3$ is greater than that of the sample with $x = 0.2$. When the sample with $x = 0.2$, the resistance value is the smallest, and the ionic conductivity is the maximum $(3.7 \times 10^{-4}\,S\,cm^{-1})$, which is higher than our previous works. The maximum conductivities of the two previous works are $1.7 \times 10^{-4}\,S\,cm^{-1}$ and $1.9 \times 10^{-4}\,S\,cm^{-1}$ respectively [34, 35].

4. CONCLUSIONS

Powders of cubic phase Ga-Nb dual doped LLZO were successfully synthesized by Sol Gel process at 800 °C. The single crystal particle size of the sample is about 100 nm, which can achieve low temperature densification. The ceramic can be obtained from powders at 1100 °C for 8 h. The sintering temperature is significantly lower than that of the powder synthesized via the traditional solid state reaction method (about 1200 °C). In addition, the sintering time of this work is 28 h shorter than that of the powder synthesized via the traditional solid state reaction method. $Li_{6.8-3x}Ga_xLa_3Zr_{1.8}Nb_{0.2}O_{12}$ $(0 \leq x \leq 0.3)$ ceramic samples gradually densify and reach the optimal Li^+ vacancy concentration with the addition of Ga, which is beneficial for enhancing conductivity. The sample with $x = 0.2$ has the best ionic conductivity, which is $3.7 \times 10^{-4}\,S\,cm^{-1}$ at room temperature. Ga-Nb co-doped LLZO electrolyte will supply potential application in the field for solid state batteries due to the fine grain and the excellent ionic conductivity.

REFERENCES

1. **Kim, T., Song, W., Son, D.Y., Ono, L.K., Qi, Y.** Lithium-Ion Batteries: Outlook on Present, Future, and Hybridized Technologies *Journal of Materials Chemistry A* 7 (7) 2019: pp. 2942 – 2964. https://doi.org/10.1039/c8ta10513h

2. **Manthiram, A.** An Outlook on Lithium Ion Battery Technology *ACS Central Science* 3 (10) 2017: pp. 1063 – 1069. https://doi.org/10.1021/acscentsci.7b00288

3. **Duffner, F., Kronemeyer, N., Tübke, J., Leker, J., Winter, M., Schmuch, R.** Post-Lithium-Ion Battery Cell Production and Its Compatibility with Lithium-Ion Cell Production Infrastructure *Nature Energy* 6 (2) 2021: pp. 123 – 134. https://doi.org/10.1038/s41560-020-00748-8

4. **Xie, J., Lu, Y.** A Retrospective on Lithium-Ion Batteries *Nature Communications* 11 (1) 2020: pp. 1 – 4. https://doi.org/10.1038/s41467-020-16259-9

5. **Zubi, G., Dufo-López, R., Carvalho, M., Pasaoglu, G.** The Lithium-Ion Battery: State of the Art and Future Perspectives *Renewable and Sustainable Energy Reviews* 89 2018: pp. 292 – 308. https://doi.org/10.1016/j.rser.2018.03.002

6. **Li, J., Shi, F., Liu, J., Zhu, K., Gao, T., Wang, J., Liu, J.** Soft-Rigid Sandwich-Structured Hybrid Electrolytes Based on Polymer-in-Ceramic Electrolytes for Stable-Cycle Solid-State Lithium-Metal Batteries *ChemElectroChem* 9 (19) 2022: pp. e202200658. https://doi.org/10.1002/celc.202200658

7. **Xu, B., Li, X., Yang, C., Li, Y., Grundish, N.S., Chien, P.-H., Dong, K., Manke, I., Fang, R., Wu, N., Xu, H., Dolocan, A., Goodenough, J.B.** Interfacial Chemistry Enables Stable Cycling of All-Solid-State Li Metal Batteries at High Current Densities *Journal of the American Chemical Society* 143 (17) 2021: pp. 6542 – 6550. https://doi.org/10.1021/jacs.1c00752

8. **Yang, H., Zhang, B., Jing, M., Shen, X., Wang, L., Xu, H., Yan, X., He, X.** In Situ Catalytic Polymerization of a Highly Homogeneous PDOL Composite Electrolyte for Long-Cycle High-Voltage Solid-State Lithium Batteries *Advanced Energy Materials* 12 2022: pp. 2201762. https://doi.org/10.1002/aenm.202201762

9. **Feng, J., Wang, L., Chen, Y., Wang, P., Zhang, H., He, X.** PEO Based Polymer-Ceramic Hybrid Solid Electrolytes: A Review *Nano Convergence* 8 2021: pp. 1 – 12. https://doi.org/10.1186/s40580-020-00252-5

10. **Wu, Y., Li, Y., Wang, Y., Liu, Q., Chen, Q., Chen, M.** Advances and Prospects of PVDF Based Polymer Electrolytes *Journal of Energy Chemistry* 64 2022: pp. 62 – 84. https://doi.org/10.1016/j.jechem.2021.04.007

11. **Balakrishnan, N.T., Das, A., Jishnu, N.S., Ahn, J.H., Jabeen, F.M., Raghavan, P.** Polyacrylonitrile (PAN)-Based Polymer Electrolyte for Lithium-Ion Batteries //Polymer Electrolytes for Energy Storage Devices *CRC Press* 2021: pp. 149 – 165. https://doi.org/10.1201/9781003144793-7

12. **Hosseinioun, A., Nürnberg, P., Schönhoff, M., Diddens, D., Paillard, E.** Improved Lithium Ion Dynamics in Crosslinked PMMA Gel Polymer Electrolyte *RSC Advances* 9 (47) 2019: pp. 27574 – 27582. https://doi.org/10.1039/c9ra05917b

13. **Li, J., Zhu, K., Wang, J., Yan, K., Liu, J., Yao, Z., Xu, Y.** Optimisation of Conductivity of PEO/PVDF-Based Solid Polymer Electrolytes in All-Solid-State Li-Ion Batteries *Materials Technology* 37 (4) 2022: pp. 240–247. https://doi.org/10.1080/10667857.2020.1827873

14. **Sun, H., Kang, S., Cui, L.** Prospects of LLZO Type Solid Electrolyte: From Material Design to Battery Application *Chemical Engineering Journal* 2022: pp. 140375. https://doi.org/10.1016/j.cej.2022.140375

15. **Nguyen, H.L., Luu, V.T., Nguyen, M.C., Kim, S.H., Nguyen, Q.H., Nungu, N.I., Jun, Y.S., Ahn, W.** Nb/Al Co-Doped $Li_7La_3Zr_2O_{12}$ Composite Solid Electrolyte for High-Performance All-Solid-State Batteries *Advanced Functional Materials* 32 (45) 2022: pp. 2207874. https://doi.org/10.1002/adfm.202207874

16. **Raju, M.M., Altayran, F., Johnson, M., Wang, D., Zhang, Q.** Crystal Structure and Preparation of $Li_7La_3Zr_2O_{12}$ (LLZO) Solid-State Electrolyte and Doping Impacts on the Conductivity: An Overview *Electrochem* 2 (3) 2021: pp. 390–414. https://doi.org/10.3390/electrochem2030026

17. **Sharifi, O., Golmohammad, M., Soozandeh, M., Oskouee, M.** Effects of Al Doping on the Properties of $Li_7La_3Zr_2O_{12}$ Garnet Solid Electrolyte Synthesized by Combustion Sol-gel Method *Iranian Journal of Materials Science and Engineering* 19 (3) 2022: pp. 1–10. https://doi. org/10.22068/ijmse.2631

18. **Birkner, N., Li, C., Estes, S.L., Brinkman, K.S.** Gallium-Doping Effects on Structure, Lithium-Conduction, and Thermochemical Stability of $Li_{7-3x}Ga_xLa_3Zr_2O_{12}$ Garnet-Type Electrolytes *ChemSusChem* 14 (12) 2021: pp. 2621–2630. https://doi.org/10.1002/cssc.202100526

19. **Gao, J., Zhu, J., Li, X., Li, J., Guo, X., Li, H., Zhou, W.** Rational Design of Mixed Electronic-Ionic Conducting Ti-Doping $Li_7La_3Zr_2O_{12}$ for Lithium Dendrites Suppression *Advanced Functional Materials* 31 (2) 2021: pp. 2001918. https://doi.org/10.1002/adfm.202001918

20. **Zhang, C., Hu, X., Nie, Z., Wu, C., Zheng, N., Chen, S., Yang, Y., Wei, R., Yu, J., Yang, N., Yu, Y., Liu, W.** High-Performance Ta-Doped $Li_7La_3Zr_2O_{12}$ Garnet Oxides with AlN Additive *Journal of Advanced Ceramics* 11 (10) 2022: pp. 1530–1541. https://doi.org/10.1007/s40145-022-0626-y

21. **Ohta, S., Kobayashi, T., Asaoka, T.** High Lithium Ionic Conductivity in the Garnet-Type Oxide $Li_{7-x}La_3(Zr_{2-x}, Nb_x)O_{12}$ (x= 0–2) *Journal of Power Sources* 196 (6) 2011: pp. 3342–3345. https://doi.org/10.1016/j.jpowsour.2010.11.089

22. **Buannic, L., Orayech, B., Lopez Del Amo, J.M., Carrasco, J., Katcho, N.A., Aguesse, F., Manalastas, W., Zhang, W., Kilner, J., Llordés, A.** Dual Substitution Strategy to Enhance Li^+ Ionic Conductivity in $Li_7La_3Zr_2O_{12}$ Solid Electrolyte *Chemistry of Materials* 29 (4) 2017: pp. 1769–1778. https://doi.org/10.1021/acs.chemmater.6b05369

23. **Košir, J., Mousavihashemi, S., Wilson, B.P., Rautama, E.L., Kallio, T.** Comparative Analysis on the Thermal, Structural, and Electrochemical Properties of Al-Doped $Li_7La_3Zr_2O_{12}$ Solid Electrolytes through Solid State and Sol-Gel Routes *Solid State Ionics* 380 2022: pp. 115943. https://doi.org/10.1016/j.ssi.2022.115943

24. **Wang, S., Chiu, H., Demopoulos, G.P.** Crystallization of Nanoscale Garnet-Type Li-Ion Conductors for All-Solid-State Batteries (ASSBs)[C]//Conference of Metallurgists. Springer, Cham. 2023: pp. 255–258.

25. **Kim, M., Kim, G., Lee, H.** Tri-Doping of Sol–Gel Synthesized Garnet-Type Oxide Solid-State Electrolyte *Micromachines* 12 (2) 2021: pp. 134. https://doi.org/10.3390/mi12020134

26. **Janani, N., Ramakumar, S., Dhivya, L., Deviannapoorani, C., Saranya, K., Murugan, R.** Synthesis of Cubic $Li_7La_3Zr_2O_{12}$ by Modified Sol–Gel Process *Ionics* 17 (7) 2011: pp. 575–580. https://doi.org/10.1007/s11581-011-0611-x

27. **Thangadurai, V., Pinzaru, D., Narayanan, S., Baral, A.K.** Fast Solid-State Li Ion Conducting Garnet-Type Structure Metal Oxides for Energy Storage *The Journal of Physical Chemistry Letters* 6 (2) 2015: pp. 292–299. https://doi.org/10.1021/jz501828v

28. **Ni, L., Wu, Z., Zhang, C.** Effect of Sintering Process on Ionic Conductivity of $Li_{7-x}La_3Zr_{2-x}Nb_xO_{12}$ (x= 0, 0.2, 0.4, 0.6) Solid Electrolytes *Materials* 14 (7) 2021: pp. 1671. https://doi.org/10.3390/ma14071671

29. **Buschmann, H., Dölle, J., Berendts, S., Kuhn, A., Bottke, P., Wilkening, M., Heitjans, P., Senyshyn, A., Ehrenberg, H., Lotnyk, A., Duppel, V., Kienle, L., Janek, J.** Structure and Dynamics of the Fast Lithium Ion Conductor "$Li_7La_3Zr_2O_{12}$" *Physical Chemistry Chemical Physics* 13 (43) 2011:pp. 19378–19392. https://doi.org/10.1039/c1cp22108f

30. **Imagawa, H., Ohta, S., Kihira, Y., Asaoka, T.** Garnet-Type $Li_{6.75}La_3Zr_{1.75}Nb_{0.25}O_{12}$ Synthesized by Coprecipitation Method and Its Lithium Ion Conductivity *Solid State Ionics* 262 (1) 2014: pp. 609–612. http://dx.doi.org/10.1016/j.ssi.2013.10.059

31. **Wu, J., Pang, W., Peterson, V.K., Wei, L., Guo, X.** Garnet-Type Fast Li-Ion Conductors with High Ionic Conductivities for All-Solid-State Batteries *ACS Applied Materials & Interfaces* 9 (14) 2017: pp. 12461–12468. https://doi.org/10.1021/acsami.7b00614

32. **Kokal, I., Somer, M., Notten, P.H.L., Hintzen, H.T.** Sol–Gel Synthesis and Lithium Ion Conductivity of $Li_7La_3Zr_2O_{12}$ with Garnet-Related Type Structure *Solid State Ionics* 185 (1) 2011: pp. 42–46. https://doi.org/10.1016/j.ssi.2011.01.002

33. **Thangadurai, V., Weppner, W.** Effect of Sintering on the Ionic Conductivity of Garnet-Related Structure $Li_5La_3Nb_2O_{12}$ and In-and K-Doped $Li_5La_3Nb_2O_{12}$ *Journal of Solid State Chemistry* 179 (4) 2006: pp. 974–984. https://doi.org/10.1016/j.jssc.2005.12.025

34. **Li, J., Zhu, K., Zhang, X., Wang, T., Li, X., Wang, J., Yan, K., Liu, J.** Effect of Ga-Bi Co-Doped on Structural and Ionic Conductivity of $Li_7La_3Zr_2O_{12}$ Solid Electrolytes Derived from Sol–Gel Method *Journal of Electronic Materials* 48 2019: pp. 7762–7768. https://doi.org/10.1007/s11664-019-07607-7

35. **Wang, T., Zhang, X., Yao, Z., Li, J., Zhu, K., Wang, J., Yan, K.** Processing and Enhanced Electrochemical Properties of $Li_7La_3Zr_{2-x}Ti_xO_{12}$ Solid Electrolyte by Chemical Co-precipitation *Journal of Electronic Materials* 49 2020: pp. 4910–4915. https://doi.org/10.1007/s11664-020-08221-8